Journal of Engineering and Sustainable Development
Vol. 30, No. 06, November 2026
https://jeasd.uomustansiriyah.edu.iq/index.php/jeasd
ISSN 2520-0917
Research Article
https://doi.org/10.31272/jeasd.2993

Land Cover Classification of Mosul Planning Using the Gray Wolf Algorithm

Joanna Hussein Yahya[1*], Almas Ahmed Khaleel[2]

[1]Department of Computer and Information Engineering, Electronics Engineering College, Ninevah University, Mosul, Iraq
[2]Department of Mathematics, College of Basic Education, University of Mosul, Mosul, Iraq

[*]Email: joanna.abdulhakeem@uoninevah.edu.iq

Article Info

Received 12/09/2024
Revised 20/10/2026
Accepted 24/10/2026

Abstract

The land cover is constantly affected by natural factors such as floods, earthquakes, and fires, as well as human activities like wars and population displacement. In this paper, a new technique is presented for classifying the land cover in the Mosul province using the Gray Wolf Algorithm (GWA). The research objective is to increase the classification accuracy rate and the efficiency of land cover classification in the Mosul planning region by using the GWA's abilities. The research improves land cover classification performance, which advances remote-sensing wisdom applications. The findings of this study present an accurate method for detailed domain classification that can be used for various land management scenarios involving environmental planning. Swarm intelligence emerges as a strategic research tool for geographic and ecological investigations because it shows effectiveness in analyzing large-scale land surface types. The GWA was implemented using MATLAB, and five classes were identified from the image. Each class (water, soils, outcrops, slope deposits, and accumulation glaciers) had a specific color to serve as a class indicator. Good results were obtained, and the accuracy was calculated after comparing it with real data, yielding 90.56%.

Keywords: Classification, Gray wolf algorithm, Image processing, Land cover.

1. Introduction

The categorization of land cover plays a significant role in the management of land use, as it furnishes researchers with crucial data on alterations occurring in land cover, such as urbanization, deforestation, and agricultural expansion [1]. The potential hazards linked with natural disasters, such as floods, wildfires, and landslides, have also been identified. Accurate classification of land cover classes enables better implementation of strategies to reduce the impact of a disaster and enables quick evacuation and rescue operations [2]. However, one of the most important artificial intelligence technologies used in classification is the swarm algorithm. The gray wolves' method suggested in 2014 by Mirjalili Seyeali is currently a prominent challenge in the world of swarm intelligence, particularly in the field of image classification. The method comes from the gray wolf behavior in nature. The structure of this method is classified into four primary levels, namely alpha (α), beta (β), delta (δ), and omega (ω), as shown in Fig. 1 [3]. The wolf α assumes the role of the group's leader and is sometimes referred to as the dominant wolf due to it taking charge of decisions relating to hunting, choosing sleeping locations, determining wake-up times, and other related matters.

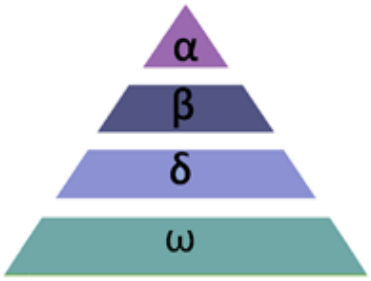

Figure 1. Hierarchy of gray wolf [3].

The pack should adhere to its order. β wolves and δ wolves are the two most well-suited individuals [4]. After completing the encirclement of the prey and during the hunting process, they will respond by helping the α wolves manage the gray wolves and make decisions. They are also candidates for α wolves [5]. The beta wolf should exhibit deference towards the alpha, while also exerting authority over the subordinate wolves. The delta wolves are required to submit to both the alpha and beta, but they hold dominance over the omega, which represents the

Work of This Research is Licensed under CC BY

lowest rank in the pack hierarchy. It is significant to note that the number of gray wolves in this category is rather small. The omega wolves consistently submit to all the other dominant wolves in the pack. It serves as a scapegoat. The final wolves were permitted to consume the omega [6]. Although omega may initially seem insignificant within the group, its absence would lead to significant issues and internal conflict within the entire pack.

Many papers have been published concerning the use of artificial intelligence for cover classification in recent years [7]. For instance:

In the same manner, Kapoor et al. [8] applied the GWA for satellite image segmentation, and while the authors modified the GWA, it was for auto-clustering entirely. This procedure was shown to increase the accuracy of estimations; it also reduced the amount of time taken for computation, as was demonstrated by their experiment done on images of New Delhi.

Liu et al. [9] performed a simulation to examine the gray wolf optimizer algorithm. It was discovered that by augmenting the dynamic weight, the alpha wolf may effectively guide the other members of the pack, greatly enhancing the algorithm's capacity to adjust to different environmental situations. The experimental findings indicate that the enhanced feed-forward neural network employs the GWO algorithm. Overcame its previous version in terms of performance.

Later, Yao et al. [10] proposed another GWA, improved gray wolf optimization (IGWO), which focused on threshold selection using the Kapur partition function. This improvement was done to eradicate previous lacunas and delivered superior optimization results.

Bansal and Singh [11] discussed the enhanced version of the classical GWO using explorative equations and opposition-based learning (OBL). The results showed the preference and superiority of the improved algorithm over other optimization techniques.

Mustafa et al. [12] used image processing techniques and remote sensing data analysis to assess the pollution of the Al-Khoser River in Mosul. Through image processing and remote sensing data analysis of Landsat ETM+ (2000) and Landsat OLI (2015) satellite images over 15 years. ERDAS image software was used to carry out supervised classification methods for detecting polluted zones while investigating land cover transformations. The analysis demonstrated explosive growth in polluted water areas because they expanded from 4.139 km^2 in 2000 to 21.45 km^2 in 2015. The satellite imagery revealed major land cover modifications when agriculture increased from 22.818 km^2 to 263.89 km^2, while uncontaminated water areas dropped from 188.77 km^2 to 155.74 km^2. The survey recorded a considerable rise in bedrock area, starting from 6.3513 km2 to 197.78 km2, while barren land expanded from its initial measurement of 36.828 km^2 to 193.53 km^2. The research results indicate that the Al-Khoser River pollution situation has deteriorated due to excessive household and industrial waste, along with decreased rainfall amounts and inadequate sewage management and water change detection capabilities, per the study, which advocates artificial intelligence and deep learning approaches for exact water quality assessment and contamination identification.

Ullah et al. [13] presented how changes in land use and land cover (LULCC) affect biodiversity and ecosystem functions in the Marghazar Valley of Swat District, Pakistan. Their findings indicate an accuracy of 91% in assessing the impacts of LULCC. Furthermore, the study focuses on the critical relationship between land use changes and biodiversity, emphasizing the need for awareness and action to mitigate the negative impacts of human activities on wildlife and ecosystems.

Sarma and Nidamanuri [14] evaluated drone-based high-resolution hyperspectral imaging for cropping identification accuracy of cabbage along with tomato and eggplant through an examination of subtle plant variations and diverse backgrounds. The developed methodology included statistical protocols alongside swarm intelligence algorithms, which determined 15 optimal bands within the 450 to 650 nm and 850 to 950 nm spectral ranges to reach classification accuracy above 93% while maintaining an F1 score of 0.93 and a kappa coefficient of 0.9. The selected bands performed as well as full-spectrum imagery and required less data processing, while providing reliable crop detection across varied sensor conditions and flight heights. The authors advocate conducting extended research that adds multiple crop types across multiple sites through active learning methods to develop advanced smart agricultural solutions.

Nagaraju et al. [15] analyzed the significance of using remote sensing imagery with Land Use Land Cover Classification (LULCC) for building land-use databases and environmental modeling. This work uses Dual Strategy-Based Bald Eagle Search (DSBES) with stacked Long Short-Term Memory (LSTM) and residual connections to tackle accuracy reduction from high-dimensional spectra by proposing a new combined methodology. DSBES better selects relevant features through its algorithm, and stacked LSTM layers analyze complicated time-based data more effectively; the integration of residual connections improves training speed by preventing gradient disappearance. The model tested across the University of California, Merced dataset (UCM), Aerial Image Dataset (AID), Northwestern Polytechnical University (NWPU) dataset, and European Satellite Dataset (EuroSAT) achieved the best accuracy of 99.71% while surpassing the results of VGG19 and Optimal Guidane Whale Optimization Algorithm-Bidirectional Long Short- Term Memory (OG-WOA-BiLSTM) classical models. The method proves efficient for improving LULC classification in conjunction with remote sensing analysis. The summary of previous literature reviews is shown in Table 1.

This work focuses on Nineveh province, located in the northern portion of Iraq. The location is approximately situated 390 kilometers north of Baghdad, between the longitudinal lines (36° 50' 53.10") and (36° 50' 20.70") north, as shown in Fig. 2. The main source of primary data is captured by the Landsat 7 Enhanced Thematic Mapper Plus (ETM+) sensor. Landsat 7 delivers data as 8-bit imagery with 256 gray levels and consists of eight spectral bands. The first three bands are within the

visible spectrum range. The fourth is for near-infrared, the fifth is dedicated to short-infrared, the sixth band is for thermal, the seventh is for mid-infrared, and the eighth is for panchromatic.

The sixth band has been omitted from the processing as it does not fit within the parameters of the land cover classification. Additionally, the last band is not utilized because of its differing spatial resolution compared to other bands. Table 2 provides a visual representation of the Landsat 7 Thematic Mapper Plus (ETM+), including the various types of bands, their corresponding wavelength in micrometers, and the resolution in meters [16].

This study presents a supervised approach for land cover categorization in Mosul planning, employing the gray wolf optimization algorithm [17]. The study is structured as follows: In Section 2, the outlined protocol for the gray wolf algorithm is presented. The procedure of the algorithm is described in Section 3. In Section 4, the procedure of the land cover categorization is illustrated. The results and discussion are presented in Section 5. Then, the limitations are provided in Section 6. Finally, the conclusion is discussed in Section 7.

Table 1. The summary of literature reviews.

References Source	Technique Used	Classification Accuracy	Research Gap
[8] Kapoor et al. (2017)	Gray Wolf Optimizer (GWO)	Improvements in accuracy regarding traditional clustering methods	Inefficiency in conventional clustering methods with non-linear data distributions.
[9] Liu et al. (2019)	Gray Wolf Optimizer (GWO)	Better classification accuracy	The evaluation focuses on resolving performance evolution capability issues that exist with conventional optimization algorithms
[10] Yao et al. (2019)	Improved Gray Wolf Optimization (IGWO)	Better segmentation results	Requires exploration to avoid local trap issues and speed optimization.
[11] Bansal and Singh (2021)	Gray Wolf Optimizer (GWO)	Enhances exploration and performance in the optimization of multi-domain applications.	Requires performance improvements
[12] Mustafa et al. (2023)	Image processing and remote monitoring with Landsat ETM+ and OLI data.	The emphasis is on recognizing pollutants and land use changes.	Advanced AI approaches are required to detect pollution more accurately and identify its source.
[13] Ullah et al. (2024)	Landsat satellite imagery to analyze and monitor fluctuations in land cover.	The focus was on investigating the impacts of land cover changes on avian populations,	Requires more investigation, especially given the growing human activity.
[14] Sarma and Nidamanuri (2025)	Hybrid algorithms (swarm intelligence and statistical methods).	With a kappa value of 0.9 and an F1 score of 0.93, classification accuracy was higher than 93%.	Limited studies on spectral band reduction using drones
[15] Nagaraju et al. (2025)	Dual Strategy-Based Bald Eagle Search (DSBES) to improve Land Use Land Cover (LULC) classification.	99.71% (UCM), 98.66% (AID), 97.59% (NWPU), and 99.24% (EuroSAT).	Addressing issues of irrelevant features, reducing computational time, and overcoming vanishing gradient problems.

Table 2. Landsat 7 Enhanced Thematic Mapper Plus (ETM+).

Band	Spectral Type	Wavelength (Micrometers)	Spatial Resolution (Meters)
1	Visible (Blue)	0.45 -- 0.52	30
2	Visible (Green)	0.52 -- 0.60	30
3	Visible (Red)	0.63 -- 0.69	30
4	Near-Infrared	0.77 -- 0.90	30
5	Shortwave Infrared	1.55 -- 1.75	30
6	Thermal Infrared	10.40 -- 12.50	60
7	Mid-Infrared	2.08 -- 2.35	30
8	Panchromatic	0.52 -- 0.90	15

Figure 2. Study area.

2. Gray Wolf Algorithm

The gray wolf algorithm is a collaborative search approach that mimics the behavior of a group of gray wolves hunting together in nature. In order to streamline the search process, wolves divide their tasks for locating prey in the following ways [18]

- Tracking for prey
- Encircling
- Attacking prey.

The Gray Wolf Optimization (GWO) algorithm emulates the predatory behavior of gray wolves to iteratively predict the whereabouts of prey. At first, a group of wolves is generated randomly, with each wolf representing a possible solution. These wolves, like their real counterparts, jointly determine the best solution (the prey) over a series of iterations. During the process, three search agents, specifically termed alpha, beta, and delta, are utilized to update the positions of the remaining wolves in the population [19] that show the highest potential. To mimic the wolves' cooperation and gain knowledge from superior search agents, let's consider a problem represented by an equation. We will start by randomly assigning places to the wolves within the search space, represented by initial $x1$ and $x2$ values.

The objective of this approach is to achieve convergence towards the best solution for the specified problem and attain the minimum values of $x1$ and $x2$, within the range of zero and one. First, define the population, specifically the number of wolves within the group, along with the frequency at which the procedure is iterated. The second phase involves determining the alpha wolf as well as the beta and gamma wolves. Subsequently, the fitness of each wolf is assessed, with the alpha wolf having the highest fitness, the beta wolf having the second highest fitness, and the gamma wolf having the third highest fitness. The third step involved the primary loop, which consisted of a collection of accounts in each individual iteration. This loop was responsible for updating the position of the wolves according to their encircling behavior, as outlined below:

$$\vec{D} = \left|\vec{C} \cdot \vec{A}_p(t) - \vec{A}(t)\right| \quad (1)$$

$$\vec{A}(t+1) = \left|\vec{A}_p(t) - \vec{B} \cdot \vec{D}\right| \quad (2)$$

where t represents the current iteration $\vec{B}$ and $\vec{C}$ are coefficient vectors, $\vec{A}_p$ is the location vector of the prey, and $\vec{A}$ denotes the position vectors of a gray wolf. The vectors $\vec{B}$ and $\vec{C}$ are obtained using the following:

$$\vec{B} = 2\vec{a} \cdot \vec{r}_1 - \vec{a} \quad (3)$$

$$\vec{C} = 2 \cdot \vec{r}_2 \quad (4)$$

The value of $\vec{a}$ vector is continuously reduced from 2 to 0 during a period of repetitions. The vectors $\vec{r}_1$ and $\vec{r}_2$ are random vectors within the range [0, 1]. We calculate the values of x_1, x_2, and x_3, since it is currently unknown which value represents alpha, beta, and gamma. We obtain a new value for x. This new value must fall within the range of 0 to 1. We then compare this new result with the previous value. If the new result is smaller, it replaces the alpha value; otherwise, it remains the same [20], [21]. Once wolves' positions have been updated using the hunting equations and the positions of alpha, beta, and gamma, we will assess the fitness of the new positions. If the fitness of any wolf surpasses that of the leader, we shall substitute it with that wolf. Ultimately, we iterate over the main loop until the maximum number of iterations. The output will provide the solution by returning the ultimate position of alpha x_1, x_2.

The following equations are utilized to mathematically represent hunting behavior [22], [23].

$$\vec{D}_a = |\vec{C}_1 \cdot \vec{A}_a - \vec{A}|$$
$$\vec{D}_ß = |\vec{C}_2 \cdot \vec{A}_ß - \vec{A}|$$
$$\vec{D}_\delta = |\vec{C}_3 \cdot \vec{A}_\delta - \vec{A}| \quad (5)$$

$$\vec{A}_1 = \vec{A}_a - \vec{B}_1 . \vec{D}_a$$
$$\vec{A}_2 = \vec{A}_ß - \vec{B}_2 . \vec{D}_ß$$
$$\vec{A}_3 = \vec{A}_\delta - \vec{B}_3 . \vec{D}_\delta \quad (6)$$

$$\vec{A}_{(t+1)} = \left(\vec{A}_1 + \vec{A}_2 + \vec{A}_3\right) \quad (7)$$

The equations in (5) calculate the distance vectors $\vec{D}_a$, $\vec{D}_ß$, $\vec{D}_\delta$ between the current location A and the product of coefficient vectors $\vec{C}_1$, $\vec{C}_2$, $\vec{C}_3$ respectively and the positions of alpha, beta, and delta wolves ($\vec{A}_a$, $\vec{A}_ß$ and $\vec{A}_\delta$).

Equation (6) determines the recent positions of the variables alpha A_1, beta A_2, and delta A_3 by subtracting the product of the coefficient vector B_1, B_2, B_3 and the distance vector D_α, D_β, and D_δ from the existing position A.

Finally, (7) computes the new average location for the entire wolf pack by taking the average of the updated positions of the alpha, beta, and delta wolves. The current average location denotes the subsequent iteration in the process [24].

3. The Procedure of Gray Wolf Algorithm

Using the landcover classification based on the gray wolf algorithm for the provided MATLAB code can be explained in the following paragraph, which depends on the equations mentioned in section two.

The MATLAB code begins by loading the satellite image of Nineveh province, with the classes representing several categories of land cover, including Mosul Dam lakes and the Tigris River, soils, outcrops, slope deposits, and accumulation glaciers. A selection of representative samples will be collected from each land cover category together with the corresponding ground truth labels to construct the training dataset. This dataset will be used to train the gray wolf algorithm (GWA) model for land cover classification.

The specified wolf population acted as a control mechanism between searching the solution space extensively and improving the top potential solution. Insufficient wolf numbers will impede the algorithm's ability to discover a wide variety of options, which leads to incorrect solutions. Large numbers of wolves degrade computational complexity when they exceed what is necessary to achieve meaningful performance gains. Researchers selected the number of wolves through experimental observation and prior scientific studies, which we proved to yield successful land cover classification results. The final determination of itr_{max} (number of iterations) was made because it had to guarantee efficient computation while reaching optimal solutions. The target is to determine how many iterations lead to stability in classification accuracy. Multiple values were examined for their influence on outcomes until researchers determined an optimal setting that strikes an equilibrium between accuracy and computational speed. The lower bound of lb and the upper bound of ub were established by referencing the color ranges from the multispectral image that was utilized in the research. All calculations needed an 8-bit digital image range with values set between 0 and 255 to preserve image processing accuracy and maintain complete important information in the data. This spectral band selection (7, 4,2) relied on the fundamental properties and classification value of each spectral band. The green wavelength position of band 2 enables effective identification between vegetation and other land cover types. Near-infrared band 4 provides powerful visibility of vegetation patterns because plants reflect this wavelength with great intensity. The critical properties of band 7 occur in the mid-infrared spectrum, which allows it to distinguish between soil and rock features. The selected bands are used in false-color composite image creation since their characteristics improve classification results.

Implementing these limitations, it ensures that the positions of the wolves remain within a suitable range relative to the threshold borders situated between the lower and upper limits. The GWA algorithm in the main loop iterates a predetermined number of times (itr_{max}). Within each iteration, the fitness of every gray wolf is assessed using the fitness function. Subsequently, the positions of wolves are revised using the hunting equation of gray wolves, taking into account the alpha, beta, and gamma. The algorithm computes the Euclidean distances between the pixels of the image and the fitness scores for each band individually. Each pixel is allocated the class index that matches it, determined by calculating the minimum distance. The function modifies the cluster centroids ('fitness_values') by computing the average value of the pixels given to each class.

The fitness function evaluates the precision of land cover classification by computing the categorized land cover with the ground truth labels. After a suitable number of iterations, namely at the point of convergence, the gray wolf with the highest fitness level emerges as the optimal answer for land cover classification. Subsequently, this approach is implemented to categorize the full image, leading to the creation of a map that classifies the land cover.

Ultimately, the algorithm allocates a specific color to each class according to the classification outcomes and produces a map of land cover classification. To assess the classification performance, the accuracy of each class is determined by comparing the findings with pre-existing ground truth data. Alternatively, the number of properly classified data points for each category, namely water, soils, outcrops, slope deposits, and accumulation glaciers, was calculated. Subsequently, we juxtaposed this tally with the overall count of points inside each corresponding category in the picture. The result is shown as the ratio of correctly classified data points according to each category. Furthermore, the comprehensive classification's overall accuracy is assessed by comparing the aggregate count of correctly classified points to the entire count of points present in the picture.

This computation allows us to assess the image's quality and identify any potential errors or areas that might be improved. In summary, this work intends to accurately classify land cover types in the Mosul region using the GWA algorithm. The purpose is to gather important information about the distribution and spatial patterns of different land cover types, which may be utilized to enhance environmental management and land use planning. The GWA approach is shown in the flowchart given in Fig. 3.

4. Land Cover Categorization Procedure

Because multispectral photos are better than single images, we used them in our investigation. This approach allows for the extraction of characteristics without any loss of information. The multispectral images are shown in Fig. 4.

The procedure begins by reading multi-band images, which undergo a series of data pre-processing steps, including registration and enhancement to highlight certain features in the image.

Given the limitation of three dimensions, information can be assigned to the three primary colors in RGB (Red, Green, and Blue). Consequently, while dealing with multispectral images including more than three bands, the user is required to carefully choose the most pertinent bands according to their research.

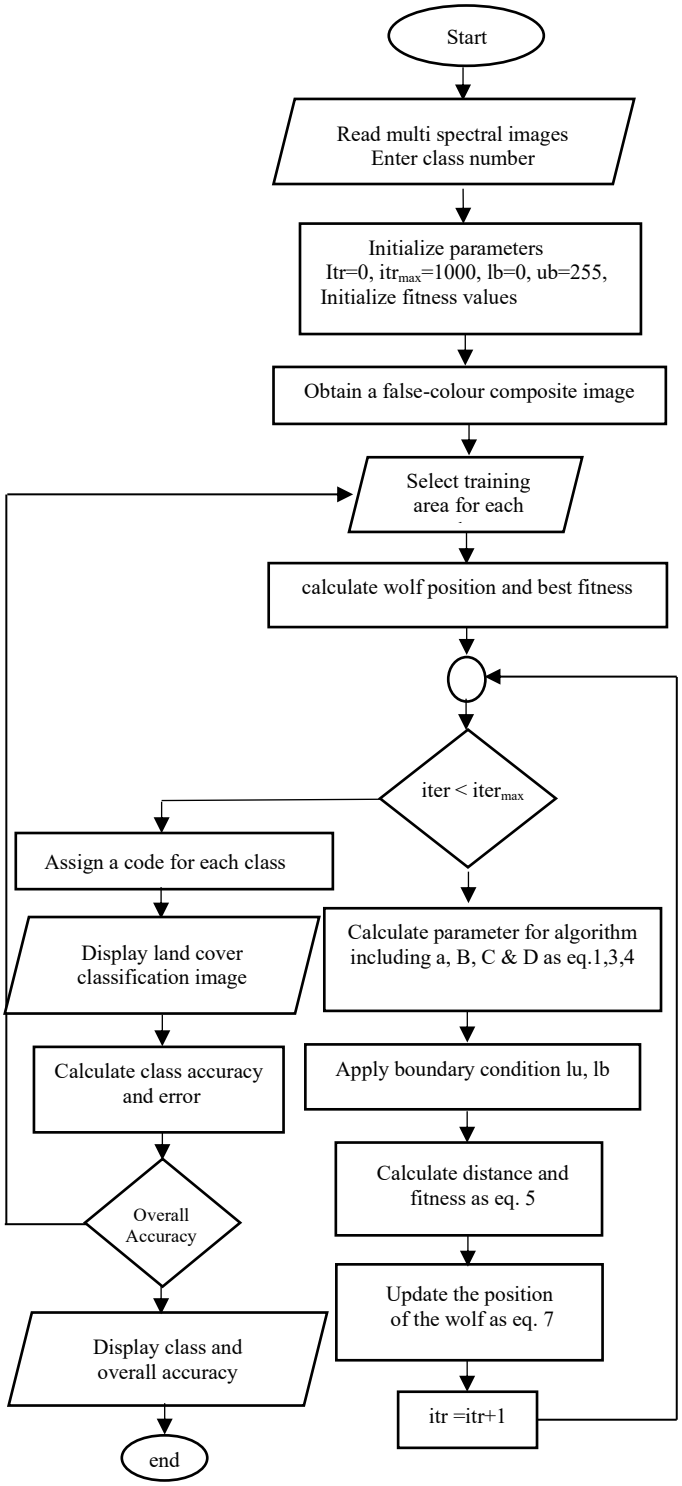

Figure 3. Flowchart of the gray wolf algorithm technique.

Each band represents one of the RGB color dimensions, creating a false-color composite image that visually represents land use based on spectral information. The spectral bands of the satellite image were combined using a 7-4-2 composition. Band 2 was selected for this sensor due to its wavelength range of 0.52-0.6 micrometers, which encompasses the portion of the electromagnetic spectrum that reflects green vegetation. Band 4, operating within the wavelength range of 0.77-0.9 micrometers, facilitates the depiction of vegetation density and distribution, hence enabling the differentiation of crops. Band 7, however, has a wavelength range of 2.09-2.35 micrometers and is crucial for distinguishing between different soil types and rocks. Consequently, the designated band arrangement is suitable for classifying land use.

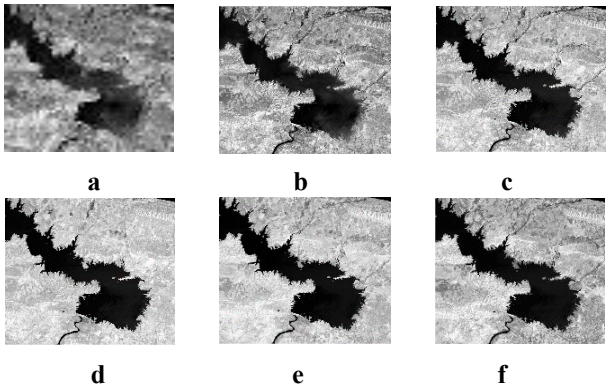

Figure 4. (a) Band 1, (b) Band 2, (c) Band 3, (d) Band 4, (e) Band 5, (f) Band 6

Through the MATLAB program, the training area received proper selection for the target classes and reference data identification. Selection of evaluation areas focused on obtaining uniform spectral distribution as well as spatial homogeneity across the image. Model accuracy necessitated a verification process for the selected data following quality assessment before performing training-testing set allocation, as shown in Fig. 5.

Figure 5. False-color composite image with band sets (7,4,2).

Fig. 6 shows the block diagram, which illustrates the steps of the land cover classification process.

5. Results and Discussion

The study introduces a land cover categorization method for Mosul planning with the Gray Wolf algorithm (GWA). The

outcome of the given code is contingent upon several aspects, including the quality of the satellite image, the precision of the

The digital classification is visually shown through the use of distinct colors to distinguish different types of land cover. The color red is used to represent the Mosul Dam lakes and Tigris River, blue indicates soils, dark green implies outcrops, light green represents slope deposits, and yellow symbolizes accumulation glacis.

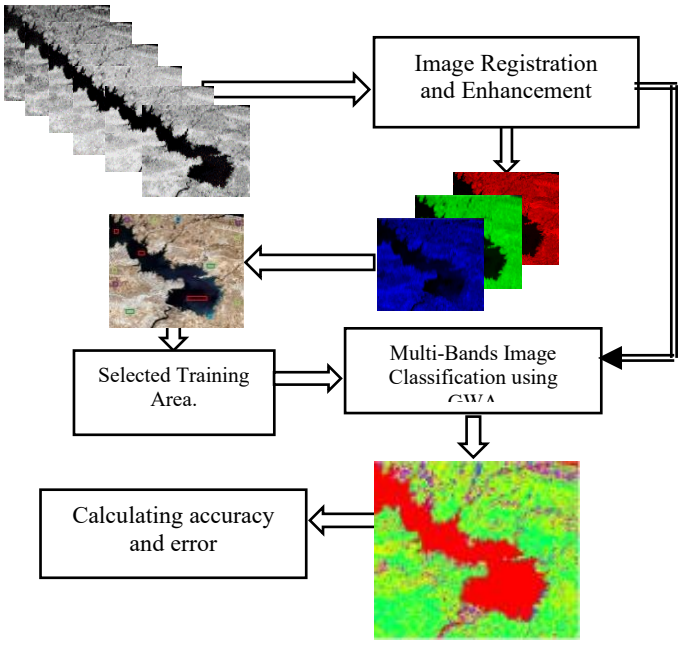

Figure 6. Land cover classification process.

The comprehension of the classification only becomes apparent when its accuracy is assessed. The primary goal of accuracy evaluation is to assess the level of exactness in the classification and to document its use in a manner that is readily comprehensible to others. The accuracy of a classification algorithm is a crucial statistic for evaluating its performance. The image classification process starts by obtaining a collection of images for which the correct categorization is already known, referred to as the "ground truth data".

Every image in this collection is paired with a specified, precise class label. Subsequently, the image classification algorithm is employed in this collection of images, providing expected class labels for each unique image. Subsequently, a comparison is undertaken between the predicted and actual class labels produced from the ground truth data. Each picture is analyzed to see whether the algorithm's prediction matches the class. The number of true positives and false positives is computed for each class, generally by generating a confusion matrix. Afterward, the accuracy rate is computed for each class separately, where a class's accuracy is the ratio of true positives to the class's total occurrences.

The overall accuracy is determined by adding up the number of true positives for each class and dividing it by the total number of instances. The mathematical expression for accuracy (ACC) is as follows:

$$\text{Acc} = \frac{\text{Sum of True Positive}}{\text{Total number of Instance}} \quad (8)$$

The classification accuracy analysis in Table 3 showed that class 1 and class 2 identified 87.50% of samples correctly, yet class 3 and class 4 reached 88.89% accuracy since the model successfully differentiated these categories. A small portion of inaccurate outcomes can be attributed to overlapping spectra. The spectral data from class 5 proved fully distinguishable because it achieved absolute accuracy of 100%. The land cover classification performance was evaluated at 93.33% using the GWA, showing a 9.44% error rate. Either training area homogeneity or reference data inaccuracies might explain this error condition. The performance quality can be boosted through enhanced preprocessing techniques along with extended spectral bands because it leads to higher classification precision and minimized class blending.

Table 3. Land cover classification result.

Class No.	Class Name	Accuracy	Error
Class 1	Water	87.50%	12.50%
Class 2	Soils	87.50%	12.50%
Class 3	Outcrops	88.89%	11.11%
Class 4	Slope deposits	88.89%	11.11%
Class 5	Accumulation glacis	100.00%	00.00%
Overall Accuracy		90.56%	9.44%

The benefits of our research compared to other studies in the literature review are the use of the Gray Wolf Algorithm (GWA) combined with remote sensing data and artificial intelligence techniques to improve land cover classification accuracy in the Mosul region, achieving 90.56% accuracy and providing accurate data for environmental planning and sustainable resource management. Fig. 7 shows the results of the image classification achieved in the context of the GWA algorithm and the identified classes that were extracted based on the processing of spectral and spatial data.

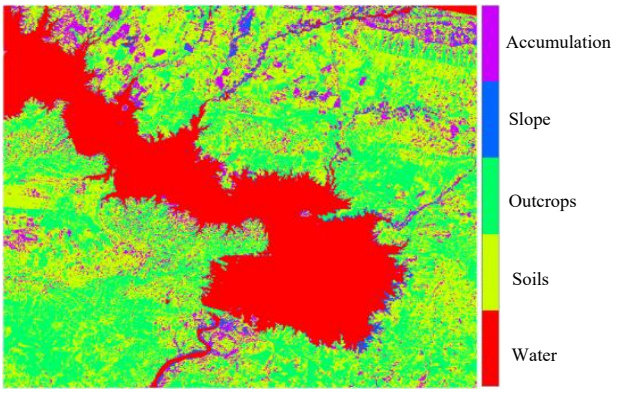

Figure 7. Image Classification Result Based on The GWA Algorithm.

6. Limitation

Under stochastic solution searches, the Gray Wolf algorithm (GWA) shows result variations in multiple runs, especially when working with complicated or dynamic data. The accuracy

rates of the gray wolf algorithm depend heavily on the selection of initial parameters, together with sample size and number of iterations, which need to be tuned specifically for peak performance. The algorithm faces difficulties in categorizing multiple groups because it uses an assumption about distinct spectral distribution patterns that natural environments sometimes fail to match. Higher-resolution images need substantial computational power, which might reduce the execution speed of the process. The performance of GWA can be improved through its combination with existing techniques and by performing direct assessments compared to alternative classification approaches during specific operational situations.

7. Conclusion

The land cover classification was performed using the Gray Wolf Algorithm in this approach. The false-color composite image was generated by merging three bands (7, 4, and 2) from the Landsat 7 Enhanced Thematic Mapper Plus (ETM+) satellite image. The precise data points were extracted from this image using field information in order to train the algorithm developed in MATLAB. The method demonstrated efficient land cover categorization of the research issue into six distinct classes: water, soil, outcrops, slope, deposit, and accumulation glacis. This research provides data that allows future studies to develop strategies for enhancing land cover classification using the gray wolf algorithm (GWA). GWA shows promise when used with support from other artificial intelligence solutions, including deep neural networks and SVM, thereby enhancing accuracy and minimizing spectral features' impact on results. An improved adaptive algorithm version would enable handling high-resolution images as well as dynamic environments to enhance result reliability throughout various areas.

The algorithm's usefulness in real-world settings would improve by developing its application to analyze multi-spectral and high-resolution datasets across broad land cover patterns. By implementing parallel computing methods and GPU acceleration to optimize performance, decrease execution time, and improve computational efficiency, the algorithm would gain increased practical value.

The study's findings promote progress toward the use of artificial intelligence for satellite image analysis to develop improved strategic planning for cities and better environmental resource management alongside natural hazard protection initiatives. The accurate development of land value in environmental change and climate model analysis.

Future work needs to test this technique on data collected from different geographical areas to determine how stable and precise the algorithm functions in various conditions.

Conflict of Interest

Regarding the publishing of this paper, the authors state that they have no conflicts of interest.

Authors Contribution Statement

Joanna H. Yahya and Almas A. Khaleel made equal contributions to each aspect of this work, doing the analysis, creating the technique, and coming up with the research proposal. The paper was written by both authors.

USE of LLM and AI

The manuscript's language, grammar, and clarity were enhanced using Grammarly and a paraphrasing tool.

Research Funding

For this study, no external financial funding was received.

Data Availability

The University of Mosul, Iraq's Remote Sensing Department, is the source of the data and satellite images used in this investigation.

Abbreviations

GWA	Gray Wolf Algorithm
GWO	Gray Optimization
ETM+	Enhanced Thematic Mapper Plus
RGB	Red Green Blue
ACC	Accuracy
t	Current repetition
$\vec{B}, \vec{C}$	Vectors of coefficient
$\vec{A}_p$	The location vector of the prey
$\vec{A}$	The position vectors of a gray wolf
$\overrightarrow{r_1}, \overrightarrow{r_2}$	A random vector within the range [0, 1]
D_α	The distance vector for alpha
D_β	The distance vector for beta
D_δ	The distance vector for delta
n	Number of wolves
lb	lower band
ub	upper band
α	Alpha gray wolf
β	Beta gray wolf
δ	Delta gray wolf
ω	Omega gray wolf

References

[1] A. Salih, "Classification and mapping of land cover types and attributes in Al-Ahsaa Oasis, Eastern Region, Saudi Arabia using Landsat-7 data," *Journal of Remote Sensing & GIS*, vol. 7, Art. no. 228, 2018. doi: https://doi.org/10.4172/2469-4134.1000228.

[2] A. Di Gregorio and L. J. M. Jansen, *Land Cover Classification System (LCCS): Classification Concepts and User Manual*, Version 1.0. Rome, Italy: Food and Agriculture Organization of the United Nations, 2000. [Online]. Available: https://www.fao.org/4/x0596e/x0596e00.htm.

[3] S. Mirjalili, S. M. Mirjalili, and A. Lewis, "Grey Wolf Optimizer," *Advances in Engineering Software*, vol. 69, pp. 46–61, 2014. doi: https://doi.org/10.1016/j.advengsoft.2013.12.007.

[4] S. Singh, S. Nikolovski, and P. Chakrabarti, "GWLBC: Gray Wolf Optimization Based Load Balanced Clustering for Sustainable WSNs in Smart City Environment," *Sensors*, vol. 22, no. 19, Art. no. 7113, 2022. doi: https://doi.org/10.3390/s22197113.

[5] R. B. Thanoon and B. A. Mitras, "Modified Grey Wolf Optimization Algorithm by using classical optimization methods," *International Journal of Computer Networks and Communications Security*, vol. 7, no.

3, pp. 49–60, Mar. 2019. [Online]. Available: https://www.proquest.com/scholarly-journals/modified-grey-wolf-optimization-algorithm-using/docview/2243313090/se-2.

[6] E. Emary, W. Yamany, A. E. Hassanien, and V. Snášel, "Multi-objective Gray-Wolf Optimization for attribute reduction," *Procedia Computer Science*, vol. 65, pp. 623–632, 2015. doi: https://doi.org/10.1016/j.procs.2015.09.006.

[7] Y. M. Abbosh, T. A. Khaleel, and J. H. Al-Khalidy, "Vegetation loss detection of Nineveh Province using remote sensing images based on Ant Colony Algorithm," *Al-Rafidain Engineering Journal*, vol. 21, no. 6, pp. 60–71, 2013. Available: https://rengj.uomosul.edu.iq/index.php/rengj/article/view/31501/31338.

[8] S. Kapoor, I. Zeya, C. Singhal, and S. J. Nanda, "A Grey Wolf Optimizer based automatic clustering algorithm for satellite image segmentation," *Procedia Computer Science*, vol. 115, pp. 415–422, 2017. doi: https://doi.org/10.1016/j.procs.2017.09.100.

[9] W. Liu, M. Hu, Z. Ye, Y. Tang, Z. Wang, L. Zhang, and L. Wei, "Feedforward neural network based on improved Gray Wolf Optimizer," in *Proc. 10th IEEE International Conference on Intelligent Data Acquisition and Advanced Computing Systems: Technology and Applications (IDAACS)*, Metz, France, Sep. 18–21, 2019, pp. 530–535. doi: https://doi.org/10.1109/IDAACS.2019.8924414.

[10] X. Yao, Z. Li, L. Liu, and X. Cheng, "Multi-threshold image segmentation based on improved Grey Wolf Optimization Algorithm," *IOP Conference Series: Earth and Environmental Science*, vol. 252, no. 4, Art. no. 042105, 2019. doi: https://doi.org/10.1088/1755-1315/252/4/042105.

[11] J. C. Bansal and S. Singh, "A better exploration strategy in Grey Wolf Optimizer," *Journal of Ambient Intelligence and Humanized Computing*, vol. 12, no. 1, pp. 1099–1118, 2021. doi: https://doi.org/10.1007/s12652-020-02153-1.

[12] F. A. Mustafa, A. A. Khaleel, and T. A. Khaleel, "Image processing approaches as a diagnostic parameter to determine pollution by using satellite imagery, Northern Iraq," *Iraqi Journal of Science*, vol. 64, no. 3, pp. 1555–1565, 2023. doi: https://doi.org/10.24996/ijs.2023.64.3.43.

[13] A. Ullah, K. Khan, N. Bibi, and S. Ahmad, "The impacts of land use change on partridge's population in the Marghazar Valley of Swat District, Pakistan," *Ornis Hungarica*, vol. 32, no. 1, pp. 16–30, 2024. doi: https://doi.org/10.2478/orhu-2024-0002.

[14] A. S. Sarma and R. R. Nidamanuri, "Optimal band selection and transfer in drone-based hyperspectral images for plant-level vegetable crops identification using statistical-swarm intelligence (SSI) hybrid algorithms," *Ecological Informatics*, vol. 86, Art. no. 103051, 2025. doi: https://doi.org/10.1016/j.ecoinf.2025.103051.

[15] V. V. Nagaraju, A. B. Jayachandra, A. Stateczny, S. H. Yogesh, R. M. Lingaraju, and B. P. B. Veeranna, "Dual strategy based improved swarm intelligence and stacked LSTM with residual connection for land use land cover classification," *IEEE Journal of Selected Topics in Applied Earth Observations and Remote Sensing*, vol. 18, pp. 4188–4198, 2025. doi: https://doi.org/10.1109/JSTARS.2024.3522197.

[16] U.S. Geological Survey, "Landsat 7 (ETM+) band designations and specifications," USGS, 2024. [Online]. Available: https://www.usgs.gov/media/images/landsat-7-band-designations.

[17] A. A. Khaleel and J. H. Al-Khalidy, "Multispectral image classification based on the Bat Algorithm," *International Journal of Electrical and Computer Engineering Systems*, vol. 13, no. 2, pp. 119–126, 2022. doi: https://doi.org/10.32985/ijeces.13.2.4.

[18] S. M. Zekavatmand, J. Vahidi, and M. B. Ghaemi, "A new way to obtain fixed point functions using the Grey Wolf Optimizer algorithm," *International Journal of Nonlinear Analysis and Applications*, vol. 14, no. 2, pp. 613–619, 2023. doi: https://doi.org/10.22075/ijnaa.2022.27491.3621.

[19] L. Korayem, M. Khorsid, and S. S. Kassem, "Using Grey Wolf Algorithm to solve the capacitated vehicle routing problem," *IOP Conference Series: Materials Science and Engineering*, vol. 83, no. 1, Art. no. 012014, 2015. doi: https://doi.org/10.1088/1757-899X/83/1/012014.

[20] A. Kumar, L. Lekhraj, S. Singh, and A. Kumar, "Grey Wolf Optimizer and other metaheuristic optimization techniques with image processing as their applications: A review," *IOP Conference Series: Materials Science and Engineering*, vol. 1136, no. 1, Art. no. 012053, 2021. doi: https://doi.org/10.1088/1757-899X/1136/1/012053.

[21] B. Sankara Babu, A. Suneetha, G. Charles Babu, Y. J. N. Kumar, and G. Karuna, "Medical disease prediction using Grey Wolf Optimization and auto encoder based recurrent neural network," *Periodicals of Engineering and Natural Sciences*, vol. 6, no. 1, pp. 229–240, Jun. 2018. doi: https://doi.org/10.21533/pen.v6i1.286.

[22] J.-S. Wang and S.-X. Li, "An improved Grey Wolf Optimizer based on differential evolution and elimination mechanism," *Scientific Reports*, vol. 9, Art. no. 7181, 2019. doi: https://doi.org/10.1038/s41598-019-43546-3.

[23] Y. Hou, H. Gao, Z. Wang, and C. Du, "Improved Grey Wolf Optimization Algorithm and application," *Sensors*, vol. 22, no. 10, Art. no. 3810, May 2022. doi: https://doi.org/10.3390/s22103810.

[24] M. H. Hashem, H. S. Abdullah, and K. I. Ghathwan, "Grey Wolf Optimization Algorithm: A survey," *Iraqi Journal of Science*, vol. 64, no. 11, pp. 5964–5984, Nov. 2023. doi: https://doi.org/10.24996/ijs.2023.64.11.40.